Subgap conductance features of $YBa_2Cu_3O_{7-\delta}$ edge Josephson junctions

A. Engelhardt, R. Dittmann, and A. I. Braginski
Institut für Schicht- und Ionentechnik, Forschungszentrum Jülich GmbH, D-52425 Jülich, Germany
(Received 7 July 1998)

The differential conductance of $YBa_2Cu_3O_{7-\delta}$ edge junctions with a $PrBa_2Cu_{2.9}O_{7-\delta}$ barrier has been investigated in detail. One striking property of our edge junctions is the existence of a well pronounced, symmetric subharmonic gap structure which is observed in the differential conductance. These features can be explained by multiple Andreev reflections if we assume the existence of a second peak in the density of states. Furthermore, a zero-bias peak in the conductivity was observed in some of the junctions, which may be explained by Andreev bound states at the interface of a *d*-wave superconductor. [S0163-1829(99)08905-5]

I. INTRODUCTION

The magnitude of the gap and the pairing symmetry in $YBa_2Cu_3O_{7-\delta}$ (YBCO) have been the subject of intensive studies. Despite the large effort invested, both are not precisely determined and clarifying experiments are still of great interest. Tunneling studies, which should yield the most direct measurement, are hampered by the difficulty of preparing high-quality tunnel junctions. Very interesting efforts in tunnel junctions with counter electrodes from conventional superconductors were performed,[1,2] but these experiments yield no information about the temperature dependence, especially at higher temperatures. Promising results for all-high-T_c tunnel junctions have been achieved with $Bi_2Sr_2CaCu_2O_{8+x}$,[3] no tunnel junctions with two YBCO electrodes have been demonstrated.

As the probability of Andreev reflections is directly related to the density of states, the differential conductance of junctions with highly transparent barriers, offers also a possibility to draw conclusions to the quasiparticle excitations.

Conventional superconductor junctions with highly transparent barriers, e.g., point contacts and microbridges, are well described by the model of Blonder, Tinkham, and Klapwijk (BTK model).[4] It is based on the theory of Andreev and normal reflection processes at the superconductor–normal conductor interfaces. Andreev reflection processes lead to the existence of an excess current at high voltages. The subharmonic gap structure at voltages $V_n = 2\Delta_S/(en)$ can be explained by multiple Andreev reflections.[5]

YBCO point contact measurements were published by different groups. Break junction measurements[6] in the point contact regime revealed a subharmonic gap structure with sharp dips at voltages $V_n = 2\Delta_S/(en)$, which can be well described by the BTK model. These results gave evidence for the existence of a true gap in YBCO single crystals and suggested a *s*-wave pairing of the superconductor.

The disadvantage of these experiments is that point contacts and break junctions have a poor reproducibility and stability. The gap value and the shape of the dI/dV curve depend on the adjustment of the sample and the measurement is sensitive to surface modifications in vacuum during the measurements.

In this work, we present measurements on edge Josephson junctions with $PrBa_2Cu_{2.9}O_{7-\delta}$ (PrBCO) barrier which have more practical relevance and exhibit well pronounced and reproducible subgap features. The transparency of the junctions is determined by the barrier material and the barrier thickness and not by sample adjustments or surface degradation during the measurement, as in the case of point contacts.

PrBCO usually is a Mott insulator,[7] but there is some evidence that it may become superconducting as well.[8] Josephson junctions with PrBCO barrier exhibit current-voltage characteristics similar to those of resistively shunted tunnel junctions, but with some significant deviations from the ideal resistively shunted junction (RSJ) model. There is strong experimental evidence that the quasiparticle transport in Josephson junctions with PrBaCO barriers occurs by resonant tunneling via 1–2 localized states, whereas the supercurrent transport occurs by direct tunneling.[9]

At least for the quasiparticles, localized states are highly transparent channels in insulating barriers. Therefore, the junction characteristics resemble more those of point contacts than those of tunnel junctions. A localized state can be described as a constriction *c* in momentum space because the resonant tunneling transport occurs only at the specific energy or momentum of the localized state. Therefore, the situation in Josephson junctions with a PrBCO barrier can be analyzed using models developed for geometrical constrictions, like the BTK model[4] where the ballistic transport can only pass a narrow channel. The phenomenological approach of the BTK model does not take into account the inelastic relaxation in the constriction region, but later microscopic calculations of Arnold[10] predicted that the position of subgap peaks is only slightly shifted from the values predicted by the BTK model. The assumption of a *s*-wave superconductor in the BTK-model is also not crucial for the application of the model for YBCO, because Devereaux *et al.*[11] showed that the peak positions persist in the case of *d*-wave symmetry and only the shape of the peaks is smeared over.

Another issue that has to be addressed is the possibility of multiple Andreev reflections in a medium where the dominating transport is resonant tunneling via localized states. The problem of the loss of phase coherence during resonant tunneling processes, especially the impact of Coulomb repulsion, has been investigated by several authors.[12,13] Golub[14] showed that, if the correlation time of the electrons in a Cooper pair is much longer than the decay time of a localized state in the conduction electron states, superconducting

correlations are not destroyed and multiple Andreev reflections are possible.

Indeed, there is clear experimental evidence for multiple Andreev reflections up to $n=8$ in a Ag-Pb/InO_x/Pb junction, with InO_x containing a high density of localized states.[15] Therefore, we can assume that Andreev reflections in PrBCO barriers are possible as well.

The observation of subgap peaks in edge junctions, which can partly be explained by BTK model have already been reported.[16,17] Furthermore, Polturak *et al.*[16] observed in some of their junctions that each subgap peak splits into three peaks at low temperatures. The data were explained by the anisotropy of the gap between *a* and *b* direction.

Here, we present detailed investigations of the subgap pattern in two different kinds of edge junctions with PrBCO barrier. One junction type contains one *ex situ* processed YBCO/PrBCO interface, while the other type has exclusively *in situ* interfaces. This allows one to distinguish between extrinsic effects related to the fabrication process and intrinsic properties of the YBCO/PrBCO interfaces.

We investigated the temperature dependence of subharmonic gap features and the influence of oxygen annealing procedures. Furthermore, we present measurements of zero-bias conductance peaks and their magnetic-field dependence. Finally, we discuss a model to describe our data in terms of an anisotropic in-plane gap in YBCO.

II. FABRICATION OF THE JOSEPHSON JUNCTIONS

Edge junctions are used in high-temperature (HT) superconducting electronics with a variety of barrier materials.[18,19] In edge junctions, the superconducting electrodes are weakly coupled along the *ab* planes via an epitaxial barrier at a shallow step in a *c*-axis-oriented YBCO film. Therefore, in contrast to the most widely used grain-boundary junctions, the current carrier transport and thus the junction properties can be influenced by the barrier thickness and the barrier material.

As the superconducting gap is expected to be direction dependent, the orientation of the junctions with respect to the crystal axis should be controlled. Therefore, we used substrates with edges oriented parallel to the (100) direction and adjusted the ramps parallel to edges of the substrates. Since YBCO films usually are twinned, the junctions may contain domains with either the *a* axis or *b* axis parallel to the ramp.

The most established way to fabricate edge junctions, which was used for our investigations as well, is to fabricate a ramp in a YBCO film by ion beam etching (see, for example, Ref. 20). The disadvantage of this method is the damage of the interface by the ion beam. This may reduce the transparency of the interface and thus influences the current carrier transport across the junction. To make a direct comparison, we additionally investigated an alternative method where the ramp is produced by a shadow mask and in the same run the barrier layer and the top YBCO electrode are deposited *in situ*.

The fabrication process for junctions fabricated *ex situ* was described in detail elsewhere.[21,22] Briefly, a bilayer consisting of a 200 nm thick YBCO film for the bottom electrode and a 200 nm thick $SrTiO_3$ insulation layer was deposited *in situ* by on-axis pulsed laser deposition (PLD). The films were patterned using standard optical lithography processes. The etching mask for the ramps consisted of conventional Hoechst AZ5214 photoresist that was softened by a 5 min post-annealing step to ensure a shallow angle. The ramp was argon-ion-beam milled by a Kaufmann-type source using an ion-beam current density of 0.25 mA/cm^2 and an accelerating voltage of 250 V. The sample was tilted 30° to the substrate normal and rotated during the etching process. This process assures a ramp angle of about 30° which prevents nucleation of grain boundaries in the subsequently deposited films.

After ion milling the ramp, a 35 min annealing step at the deposition temperature and deposition oxygen pressure was carried out in the deposition chamber to recrystallize amorphous material on the surface of the etched YBCO. Afterwards, the PrBCO barrier and another 200 nm thick YBCO film for the top electrode, were deposited *in situ* by sputtering.

The fabrication process for junctions fabricated completely *in situ* by the shadow micro-mask technique was described in detail elsewhere.[23] Briefly, a patterned 700 nm thick CaO/ZrO_2 mask is deposited and patterned on the substrate. This substrate is mounted on the heater of the deposition chamber and heated up to the deposition temperature of about 800 °C. The bottom YBCO electrode is then deposited by PLD under an angle of 45°. Due to the microshadow mask, a ramp is formed directly during the deposition without any further treatment. Therefore, the surface of the ramp is not damaged by an etching process or degraded by surface reactions during *ex situ* processing.

The PBCO barrier and the YBCO counter electrode are deposited *in situ* at normal angle of incidence. The different deposition angle insures a relatively homogeneous nominal thickness of the barrier on the ramp.

Both junction types were typically fabricated with a nominal PrBCO barrier thickness of 30–45 nm. However, the real thickness of the barrier layer is affected by thickness variations across the junction area.

The junctions themselves were defined by standard optical lithography and a second argon-ion-beam etching step. Finally, a gold layer with a thickness of 200 nm was evapo-

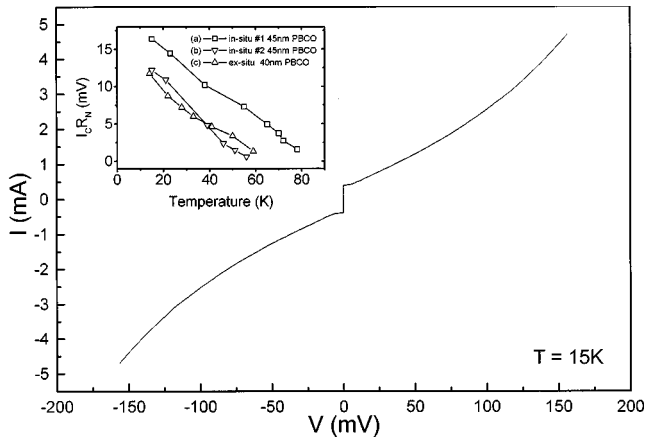

FIG. 1. *I-V* characteristic of a 3 μm-wide *in situ* junction with a 45 nm PBCO barrier at 15 K. Inset: Temperature dependence of the I_cR_N product of different *in situ* and *ex situ* junctions.

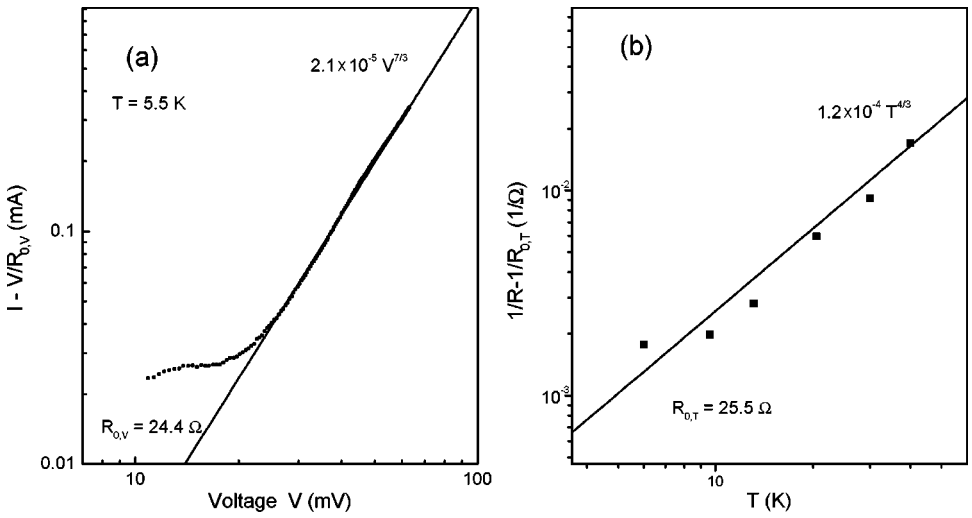

FIG. 2. (a) Double logarithmic plot of the current-voltage characteristic; the voltage independent resistance $R_0=R(V=0,T=5.5\ \mathrm{K})$ is subtracted. Solid line: Data fit using $2.1\times10^{-5}\ V^{7/3}$ dependence ($V\geqslant 25$ mV); (b) Double logarithmic plot of the temperature dependence of the voltage-independent conductance $1/R\text{-}1/R_0$, with $R_0=R(V=0,T=5.5\ \mathrm{K})$ subtracted. Solid line: Data fit using $1.2\times10^{-4}\ T^{4/3}$ dependence.

rated and patterned by a liftoff process to provide electrical contacts to the bottom and top electrode.

III. RESULTS AND DISCUSSION

The current-voltage (I-V) characteristics of the junctions were measured by four-point measurements in a liquid-helium dewar. The measurements at 0.6 K were performed in a He^3/He^4 cryostat. The differential resistance dV/dI of the junctions was measured by lock-in technique. In addition to the dc current I, the sample was biased with an ac current dI with an amplitude of about 0.2% of I with a frequency of 470 Hz. The voltage signal dV was phase-sensitively detected.

A. Current-voltage-characteristics

Figure 1 shows the I-V characteristic of an *in situ* fabricated junction with a PrBCO barrier of 45 nm at 15 K. The shape of the curve is RSJ-like with a significant contribution of excess current. The critical current I_c is 419 μA and a I_cR_N product of 16 mV could be obtained in this junction. The inset in Fig. 1 shows the temperature dependence of the I_cR_N product for two different *in situ* junctions and one *ex situ* junction with a thickness of about 40 nm. The curves are nearly linear and the magnitude at low temperatures is in the same order of magnitude as the superconducting gap. For a tunnel junction, the Ambegaokar-Baratoff relation predicts $I_cR_N\approx\pi\Delta/2e$ at $T\ll T_c$.[24] A suppression of the order parameter at the interface results in a suppression of the I_cR_N product. Therefore, in the case of our junctions, no dramatic suppression of the order parameter occurred at the YBCO-PrBCO interface.

Except for the one *in situ* junction in Fig. 1 [curve (a)], most of the *in situ* junctions showed I_cR_N products were comparable to curve (b) and exhibited no significant higher values than the investigated *ex situ* junctions [curve (c)]. Therefore, there seems to be no significant suppression of the order parameter at the interface due to the *ex situ* treatment.

A striking feature of the I-V curves of both types of junctions at lower temperatures is the increase of the conductivity with increasing voltage. According to calculations of Glazman and Matveev (GM), resonant tunneling via one and two localized states leads to[25]

$$I=[\langle G_1\rangle+\langle G_2(T,0)\rangle+\langle G_2(0,V)\rangle]\cdot V \tag{1}$$

with the different conductance contributions $\langle G_{1,2}\rangle$. Furthermore, when

$$k_BT\gg eV:\langle G_2(0,V)\rangle=A\cdot V^{4/3}, \tag{2}$$

$$k_BT\ll eV:\langle G_2(T,0)\rangle=B\cdot T^{4/3}. \tag{3}$$

The temperature- and voltage-independent part $\langle G_1\rangle$ contains contributions from elastic and inelastic tunneling via one localized state. In the case of elastic tunneling, the density of localized states can be estimated using the Larkin-Matveev results[26]

$$\langle G_1\rangle=(2e^2/h)N_e. \tag{4}$$

The temperature- and voltage-dependent parts $\langle G_2(T,0)\rangle$ and $\langle G_2(0,V)\rangle$ are contributions from resonant tunneling via two localized states.

Figure 2(a) shows that the voltage-dependent component of the current $I\text{-}V/R(V=0)=\langle G_2(0,V)\rangle\cdot V$ of an *in situ* junction which was measured up to very high bias voltages at $T=5.5$ K. For voltages above 25 mV, $I\text{-}V/R(V=0)$ is proportional to $V^{7/3}$ and fits well Eqs. (1) and (2), respectively. The fit parameters can be extracted from Table I. Therefore, above voltages comparable to the gap, the quasiparticle current in our junctions can be described by the GM model developed for normal conductor-insulator–normal conductor (NIN) junctions, with I containing localized states.

This picture holds even for lower voltages, if we analyze the temperature dependence of the conductivity. Figure 2(b) shows that the temperature-dependent part of the conductivity at low voltages $1/R(T,V=0)-1/R(0,0)=\langle G_2(T,0)\rangle$ is proportional to $T^{4/3}$ in agreement with Eq. (3).

For edge junctions with a PrBCO barrier, this temperature dependence, ascribed to resonant tunneling via one and two localized states, has been observed by several groups (Refs. 9 and 27).

The existence of a superconducting gap was not taken into account in the theory. Assuming s-wave symmetry of the order parameter, Devyatov *et al.* extended the GM model to superconducting electrodes, and showed that the low-temperature dependence of $\langle G_2\rangle$ is more exponential rather

TABLE I. Results of the Glazman-Matveev fit of the *I-V* characteristic of different samples with 40 nm PrBCO; bridge width 4 μm.

Sample	$I_c(\mu V)$	$R(V=0)$ (Ω)	G_1 $(mA/V^{7/3})$
# ldy1662			
before annealing (*in situ*)	450	24	2.1×10^{-5}
# ldy1662			
after annealing (*in situ*)	450	47	3×10^{-5}

than given by a power law.[28] This dependence could not be observed in our or by other groups junctions. A possible explanation is that due to nodes in the gap, the quasiparticle transport resembles more that in a NIN junction than in a SIS junction, with *S* being an *s*-wave superconductor.

To check the influence of the oxygen content on the transport properties, a sample was annealed using a 20 mbar oxygen plasma at a temperature of about 550 °C for 30 min. Table I shows the data before and after annealing. This treatment did not influence the critical current, but decreased the conductance $\langle G_1 \rangle$ of the junctions by a factor of 2, which is due to Eq. (4) an indication that the oxygen content changes the number of localized states in the barrier. A possible explanation is that the localized states are connected with oxygen vacancies. As no influence of the oxygen content on the critical current could be observed, the Cooper-pair current is not influenced by the number density of localized states. This suggests that the transport mechanism for Cooper pairs can not be ascribed to resonant tunneling via localized states. Similar observations have been reported by Verhoeven *et al.* who changed the Ga content in $PrBa_2Cu_{3-x}Ga_xO_{7-\delta}$, which is supposed to change the density of localized states. The Ga content influenced $\langle G_1 \rangle$ but not the critical current.[9] They conclude, supported by the different decay length for the thickness dependence of supercurrent and normal resistance, that the Cooper pair transport occurs by direct tunneling rather than by resonant tunneling via localized states. As we do not have enough systematic data for different oxygen contents and related thickness dependencies, we do not draw conclusions concerning the Cooper pair transport.

B. Subharmonic gap structure

Figure 3 shows the differential conductance of an *in situ* fabricated junction with a barrier thickness of 40 nm plotted against voltage at 5.5 K. The data points at low bias voltage are skipped because they include very high values due to the supercurrent contributions. Some of the junctions showed an additional zero-bias conductance peak which will be discussed later. The solid line in Fig. 3 is the $\langle G_2(0,V) \rangle = A \cdot V^{4/3}$ with $A=2\times10^{-5}$ fit of the background conductance corresponding to Eq. (2).

A well pronounced, symmetric subharmonic gap structure can be seen in Fig. 3. Only some of the peaks could be explained by the BTK model. Other explanations for peaks in the conductivity are geometrical resonances like Tomash and Mc-Millan oscillations which result from multiple Andreev and normal reflections between normal conducting, superconducting and insulating boundaries (see overview in the book of Wolf[29]). These geometrical resonances result in equidistant peaks and therefore do not fit our data.

A better description can be achieved if the BTK model is extended to a more complicated density of states. In the BTK model, there is only one peak in the density of states at the gap Δ_S. For a system including a proximity layer at both interfaces, Aminov *et al.*[30] showed that a second peak in the density of states at the proximity gap Δ_N result in four series of peaks in the differential conductivity. These peaks should have the voltage positions:

$$\frac{2\Delta_S}{en};\frac{2\Delta_N}{en};\frac{\Delta_S-\Delta_N}{en},\frac{\Delta_S+\Delta_N}{en}, \tag{5}$$

where *n* is the number of Andreev reflection.

In this superconductor–normal-metal-constriction–normal-metal–superconductor (SNcNS) model, the constriction is assumed to be small and ballistic, but a recent microscopic model of Zaitsev[31] predicted that the positions of the peaks persist also in the case of diffusive transport.

In Fig. 4 the positive voltage branch of the conductance measurement of Fig. 3 is shown and the visible minima of the conductance are marked. In comparison, the positions of the four series of voltages for $n=1$ and $n=2$ are shown with the two order parameters $\Delta_S=25$ meV and $\Delta_N=16$ meV. All visible peaks can be explained in this model. The values are stated in Table II. From the conductance measurements of about 20 *in situ* fabricated junctions on different chip samples, the gap values are in the range of 21–26 meV for Δ_S and of 13–17 meV for Δ_N. The *ex situ* fabricated junc-

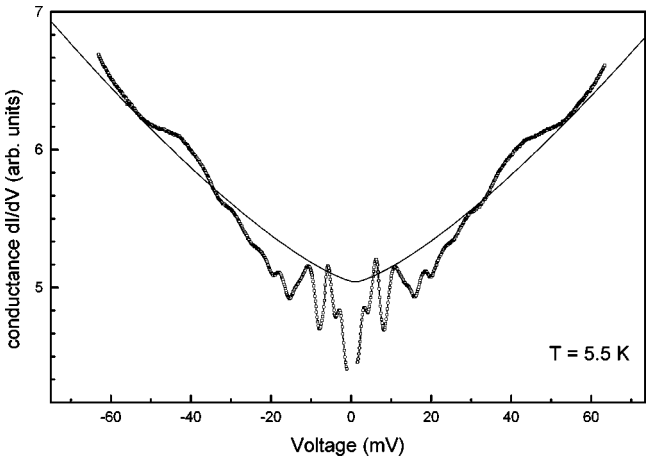

FIG. 3. Differential conductance of the junction showing a subharmonic gap structure at 5.5 K. The junction showed a supercurrent at this temperature, therefore data points at low bias voltages are not plotted. The solid line is the fit $G(V)=2.1\times10^{-5}\ V^{7/3}$ corresponding to the Glazman-Matveev theory.

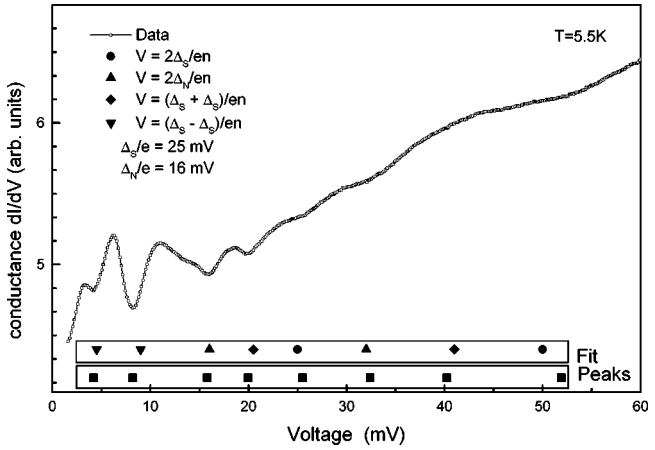

FIG. 4. Differential conductance of Fig. 3. The peaks are compared with the values of the subharmonic gap structure in the SNcNS model for $n=1$ and $n=2$.

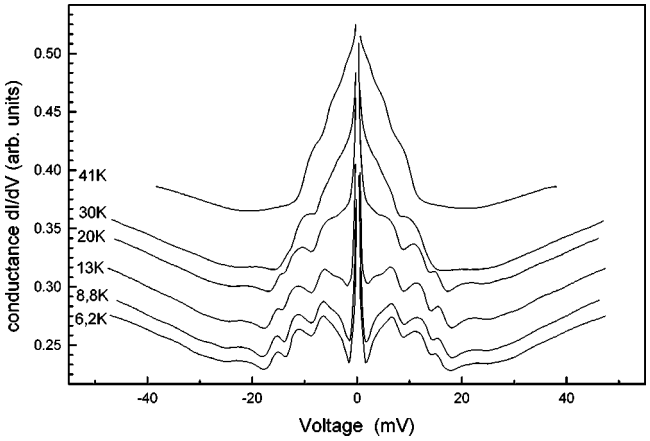

FIG. 5. Differential conductance at different temperatures. The characteristics are vertically shifted for clarity.

tions showed sharp subgap peaks as well and could be fitted to the model with comparable values for Δ_S and Δ_N.

One possible origin for Δ_N is the existence of a normal conducting layer at the interface produced by the fabrication process. In that case, the value for Δ_N should be significantly lower for the junction with the *ex situ* fabricated interfaces. As we obtained the same values for *in situ* and *ex situ* junctions, Δ_N seems to be a more fundamental property of YBCO.

The determined gap values correspond to values of $2\Delta_S/kBT_C=6.5$ and $2\Delta_N/kBT_C=4.2$. Most of the values quoted in the literature are centered around the value $2\Delta_S/kBT_C=5$.[32]

Aminov *et al.*[33] already reported the observation of a two-gap structure in YBCO single crystals with gap values at $\Delta=24$–28 meV and $\Delta=29$–30 meV. Hass *et al.*[34] reported a two-gap structure in point contacts with gap values of $\Delta=12$ meV and $\Delta=20$ meV.

In *in situ* prepared junctions, Polturak *et al.*[16] observed a splitting of the gap peak into three peaks, independent of the barrier material. The average value for the voltage positions was 16.2, 20, 24 meV. The maximum and the minimum values are nearly the same as observed in our junctions and therefore suggest the effect to be intrinsic for YBCO and not depending on the junction fabrication process or the barrier material.

TABLE II. Comparison of the peak positions with the expected values for $\Delta_S=25$ meV, $\Delta_N=16$ meV, and $n=1$, $n=2$.

Peaks (mV)	$2\Delta_S/en$, (n)	$2\Delta_N/en$, (n)	$(\Delta_S-\Delta_N)/en$, (n)	$(\Delta_S+\Delta_N)/en$, (n)
4.2				4.5, (2)
8.2				9, (1)
15.8		16, (2)		
20			20.5 (n)	
25.5	25.2, (2)			
32.4		32, (1)		
40.2			41, (1)	
51.9	50, (1)			

To obtain further information about the structures, the temperature dependence of the peak position and amplitude was investigated. The conductance at different temperatures is shown in Fig. 5. The subharmonic gap structure smears over to higher temperatures and above 30 K vanishes completely, although the critical temperature of the superconducting electrodes is about 89 K. The peaks move with increasing temperature to smaller voltages. At higher temperatures, the smaller peaks vanish into the background conductance. Flensberg *et al.*[35] calculated the temperature dependence of the subharmonics gap structure and showed that the peaks should broaden and vanish near the critical temperature. In our measurements, as well as in those of other groups,[16] the peaks disappear at much lower temperatures. This can possibly be explained by additional smearing of the subharmonic gap structures due to the presence of gap nodes in YBCO.[11]

For a junction with a proximity layer at the interfaces, Aminov *et al.* showed that with increasing temperature, the position of the peaks related to Δ_N move to higher voltages relative to the peaks which correspond to Δ_S.[30] The changing shape of our dI/dV characteristic and the smearing of the structures makes it difficult to observe this effect. Therefore, from the temperature dependence we cannot draw any conclusions concerning the origin of Δ_N.

There are several existing theories, which describe YBCO as a system containing one intrinsically normal (CuO chains) and one superconducting (CuO-planes) subsystem.[36–38] Due to the intrinsic proximity effect, superconductivity is induced in the chains. As a result, two gaps appear in the excitation spectrum at the positions Δ_a and Δ_b and can be an explanation for our data if we identify Δ_a with Δ_S and Δ_b with Δ_N. One problem with this interpretation is, that a pure proximity coupling between the planes and the chains, without any off-diagonal pairing, result in a chain gap Δ_b in the order of 0.1 meV,[39] which is two orders of magnitude lower than the Δ_b observed in our experiments. Atkinson *et al.*[39] introduced an off-diagonal pairing between the chains and the planes and obtained gap values $\Delta_S=27$ eV and $\Delta_b=17$ meV, which are in good agreement with our data. A direct consequence of this model is that the order parameter is not of a pure $d_{x^2-y^2}$ symmetry, but should contain a significant s admixture.[39]

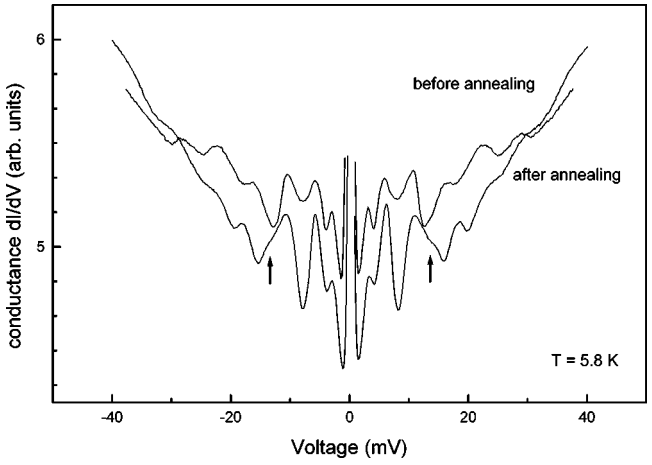

FIG. 6. Differential conductance before and after annealing in oxygen plasma at a temperature of about 550 °C for 30 min.

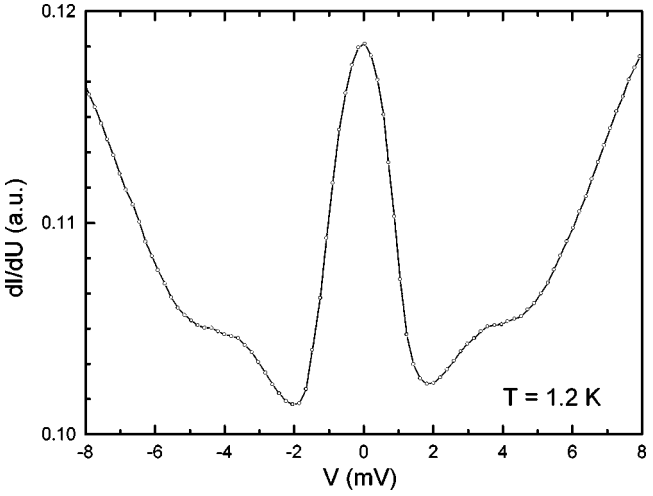

FIG. 7. Differential conductance at 1.2 K of a junction without supercurrent; barrier thickness 45 nm, junction width: 3 μm.

Within this model, the value of the gap in the CuO chains is sensitive to the oxygen content. To investigate the influence of the oxygen content on the subgap pattern, a sample was annealed for 30 min using a 20 mbar oxygen plasma at a temperature of about 550 °C. Figure 6 shows the conductance of the same junction before and after annealing. There are only slight differences in the structures. The fact that the background conductivity changes due to the reduction of the density of localized states makes it difficult to detect the change in position of the peaks at higher voltages. An obvious difference can be seen at $\Delta_N = 16$ meV marked by the arrows in Fig. 6. The minimum is shifted towards higher voltages as expected if the proximity coupling of the planes and the chains is increased by the oxygen annealing. The effect is too small to be detected in the case of the sum and difference peaks. However, the subgap pattern connected with Δ_N depends on the oxygen content as expected if Δ_N were the proximity-induced gap in the chains.

C. Zero-bias conductance peaks

Some of the investigated junctions showed at low temperatures a conductance peak at zero-bias voltage (ZBCP). The width of such a peak was between several 100 μV and several mV depending on the sample. The magnitude decreased with increasing temperature, the peak smeared over and vanished. It is difficult to investigate these peaks because of huge peaks due to the supercurrent. Due to barrier inhomogeneities, the supercurrent could not be totally suppressed by magnetic field in our junctions.

Therefore, we choose a sample with a 45 nm thick PrBCO barrier which did not show a supercurrent. This can be explained by the fact that the real thickness may be higher than the nominal thickness or at least higher than that of the other samples on the chip which showed supercurrents. The dI/dV curve of the sample at 1.2 K is shown in Fig. 7. There can be seen a striking ZBCP with a width of 2 mV.

ZBCP's were observed by several groups for tunnel junctions,[2] bicrystal junctions[40] and at YBCO-N boundaries.[41,43] The first experiments have been explained in terms of magnetic scattering centers at HT superconducting interfaces using the Appelbaum-Anderson theory.[44] Recently,[45] ZBCP's were explained by midgap Andreev bound states that are unique to *d*-wave pairing symmetry and were predicted by Hu.[46] ZBCP's should be observed in the (110) direction where incident and reflected particles change sign at the interface. In our experiments, the current direction should ideally be (100), but, due to faceting of the YBCO ramp, the formation of (110) interfaces is likely. Covington *et al.*[45] observed a ZBCP in the (100) as well as in the (110) direction.

To gain further information about the ZBCP, we cooled the sample down to 0.6 K and measured the magnetic-field dependence. We observed a significant influence of magnetic field on the shape of the ZBCP. As the magnitude of the applied field increases from 0 to 7 T, the conductance at zero bias decreases and the conductance at about ± 0.2 mV increases. That means that the spectral weight is shifted to higher energies. This is more easily observed if we plot the difference $G(H,V)$-$G(H=0,V)$ between the conductance curves at zero and high magnetic fields, as shown in Fig. 8. Two peaks can be observed, separated by the distance 2δ, the shift of the spectral weight. The inset of Fig. 8 shows the magnetic-field dependence of 2δ. At low magnetic fields, there is a strong increase of the splitting. Above a magnetic field of about 1.5 T, the slope changes and the splitting increases only slightly and linearly with the magnetic field.

The interpretation of the ZBCP's in our junctions in terms of the Appelbaum-Anderson model cannot be excluded because the quasiparticle current transport in the junctions is dominated by the existence of localized states. These localized states may be connected with localized magnetic moments. Tunneling electrons could be scattered via spin-exchange interactions, giving rise to additional conduction channels and cause ZBCP's. An applied magnetic field suppresses the tunneling conductance, and splits the peak due to Zeemann splitting. The splitting δ of the peaks should be linear with the applied magnetic field: $2\delta = 2g\mu_B H$. Here μ_B is the Bohr magneton and g is the Landé factor for the impurity spin. However, our data (see the inset of Fig. 8) would imply a magnetic-field-dependent g factor, what cannot be explained within existing models.

A similar dependence of the ZBCP on the magnetic field was observed at YBCO bicrystal junctions[40] and at YBCO-Au interfaces.[41] Furthermore, absence of ZBCP's

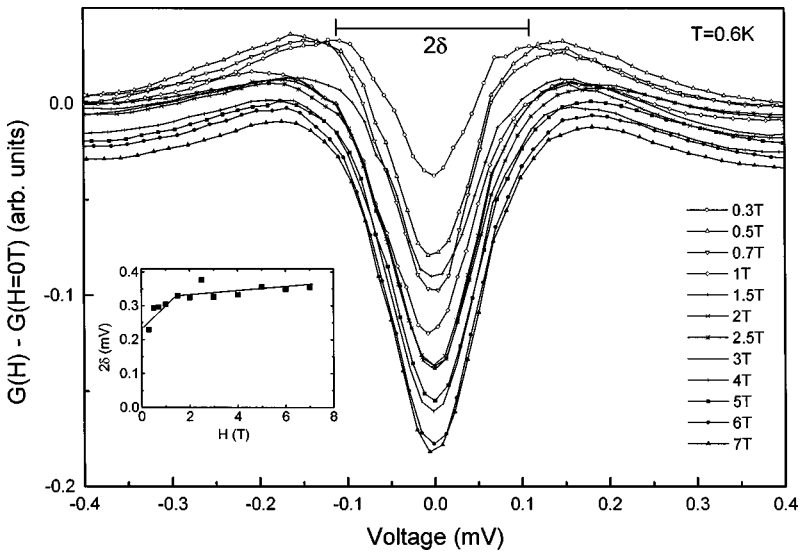

FIG. 8. Voltage dependence of $G(H)$-$G(H=0)$ at different magnetic-fields. The field is applied perpendicular to the edge junction; Inset: magnetic field dependence of 2δ; the solid line is a guide to the eye.

was reported in the case of $Nd_{1.85}Ce_{0.15}CuO_4$, which is supposed to be an *s*-wave superconductor.[42] Therefore, it is reasonable to explain the observed ZBCP's in terms of Andreev bound states connected with the *d*-wave pairing symmetry in YBCO. Fogelström *et al.* calculated the splitting of the ZBCP caused by Andreev bound states in a *d*-wave superconductor.[47] According to this model, the surface bound states couple to the magnetic field via the screening current in the superconductor. Due to the Doppler shift, the Andreev bound state is shifted. For low magnetic fields, this effect leads to a linear increase of the shift with magnetic field. There is a maximum shift when the screening current reaches the value of the order of the bulk critical current. If the field is increased above the corresponding field H_0, which should be between 1 and 10 T, the shift becomes nearly field independent. The change of the slope at a field $H_0=1.5$ T in the δ versus H dependence (inset of Fig. 8) can be well explained. One problem in the interpretation of our data is the fact that we subtracted the peak at zero magnetic fields to determine δ. Therefore, we cannot prove that there is already a splitting at zero magnetic field as was directly observed in YBCO/I/Cu tunnel junctions.[45] Fogelström *et al.*[47] attributed the zero-field splitting to the stabilization of a subdominant complex *s*-wave order parameter at the interface.

However, even if the interpretation of the magnetic-field dependences is not completely understood, there is some evidence for *d*-wave pairing in our junction.

IV. CONCLUSIONS

We investigated the I-V characteristics and the differential conductivity of YBCO edge junctions with PrBCO barrier in detail. Independent of the junction fabrication process, we obtained I_cR_N products of about 10 mV at 4.2 K. From the I-V characteristics, we were able to confirm that the quasiparticle current occurs by resonant tunneling via 1 and 2 localized states as reported previously by other groups.[9,27]

In the differential conductivity, we observed a well-pronounced subgap pattern, which is stable and independent on the junction fabrication process. This subharmonic gap pattern can be well described by multiple Andreev reflections, assuming an anisotropic in-plane gap in YBCO. From this assumption, we determined $\Delta_a=21$–26 meV and $\Delta_b=13$–17 meV which can be ascribed to the gap in the CuO_2 planes and the gap in the CuO chains, respectively. The observed gap values fit well to the model of Atkinson *et al.*,[39] who assumed an off-diagonal pairing, additional to the *d*-wave pairing in the CuO_2 planes. A direct consequence of this model is that the order parameter is not of a pure $d_{x^2-y^2}$ symmetry, but should contain a significant *s* admixture.[39]

Furthermore, we observed a ZBCP in some of our junctions. The magnetic-field dependence of the ZBCP cannot be explained in terms of magnetic impurity scattering, but can be attributed to the presence of zero energy bound states at the surface of a *d*-wave superconductor.

ACKNOWLEDGMENTS

We would like to thank S. Golubov for critically reading the manuscript. We acknowledge M. Y. Kupryanov, B. A. Aminov, and S. Lachenmann for helpful discussions and T. Schäpers for making his measurement equipment available to us.

[1] J. Geerk, X.X. Xi, and G. Linker, Z. Phys. B **73**, 329 (1988).

[2] J. Leseur, L. Greene, W.L. Feldmann, and A. Inam, Physica C **191**, 325 (1992).

[3] I. Bozovic, J.N. Eckstein, G.H. Virshup, A. Chaiken, M. Wall, R. Howell, and M. Fluss, J. Supercond. **7**, 187 (1994).

[4] G. E. Blonder, M. Tinkham, and T. M. Klapwijk, Phys. Rev. B **25**, 4515 (1982).

[5] T. M. Klapwijk, G.E. Blonder, and M. Tinkham, Physica B & C **109&110B**, 1657 (1982).

[6] Ya. G. Ponomarev, N. B. Brandt, C. S. Khi, S. V. Tchesnokov, E.

B. Tsokur, A. V. Yarygin, K. T. Yusupov, B. A. Aminov, M. A. Hein, G. Müller, H. Piel, D. Wehler, V. Z. Kresin, K. Rosner, K. Winzer, and Th. Wolf, Phys. Rev. B **52**, 1352 (1995).
[7] B. Fisher, G. Koren, J. Genossar, L. Patlagan, and E.L. Gartstein, Physica C **176**, 75 (1991).
[8] Z. Zou, K. Oka, T. Ito, and Y. Nishihara, Jpn. J. Appl. Phys., Part 2 **36**, L18 (1997).
[9] M. A. J. Verhoeven, G. J. Gerritsma, H. Rogalla, and A. A. Golubov, Appl. Phys. Lett. **69**, 848 (1996).
[10] G.B. Arnold, J. Low Temp. Phys. **59**, 143 (1985); **68**, 1 (1987).
[11] T.P. Devereaux and P. Fulde, Phys. Rev. B **47**, 14 638 (1993).
[12] L.I. Glazman and K.A. Matveev, Sov. Phys. JETP **67**, 1276 (1988).
[13] A.I. Larkin and K.A. Matveev, Sov. Phys. JETP **66**, 580 (1987).
[14] A. Golub, Phys. Rev. B **52**, 7458 (1995).
[15] A. Frydman and Z. Ovadyahu, Phys. Rev. B **55**, 9047 (1997).
[16] E. Polturak, G. Koren, D. Cohen, and E. Aharoni, Phys. Rev. B **47**, 5270 (1993).
[17] H. Predel, H. Burkhardt, and M. Schilling, Inst. Phys. Conf. Ser. **158**, 471 (1998).
[18] B.D. Hunt, M.G. Forrester, J. Tlvacchio, R.M. Young, and J.D. McCambridge, IEEE Trans. Appl. Supercond. **7**, 2936 (1997).
[19] M. Hidaka, T. Satoh, H. Terai, and S. Tahara, IEICE Trans. Electron. **E-80C**, 1226 (1997).
[20] J. Gao, Yu. M. Boguslavskij, B.B.G. Klopman, D. Terpstra, R. Wijbrans, G.J. Gerritsma, and H. Rogalla, J. Appl. Phys. **72**, 575 (1992).
[21] C. Horstmann, P. Leinenbach, A. Engelhardt, R. Dittmann, U. Memmert, U. Hartmann, A.I. Braginski, IEEE Trans. Appl. Supercond. **7**, 2844 (1997).
[22] C. Horstmann, P. Leinenbach, A. Engelhardt, R. Gerber, C.L. Jia, R. Dittmann, U. Memmert, U. Hartmann, and A.I. Braginski, Physica C **302**, 176 (1998).
[23] M.D. Strikovskiy and A. Engelhardt, Appl. Phys. Lett. **69**, 2918 (1996).
[24] V. Ambegaokar and A. Baratoff, Phys. Rev. Lett. **11**, 486 (1962).
[25] L.I. Glazman and K.A. Matveev, Sov. Phys. JETP **67**, 1276 (1988).
[26] A.I. Larkin and K.A. Matveev, Sov. Phys. JETP **66**, 580 (1988).
[27] T. Satoh, M.Y. Kupriyanov, J.S. Tsai, M. Hidaka, and T. Tsuge, IEEE Trans. Appl. Supercond. **5**, 2612 (1995).
[28] I.A. Devyatov and M.Yu. Kupriyanov, JETP **65**, 174 (1997).
[29] E.L. Wolf, *Principles of Electron Tunneling Spectroscopy* (Oxford, New York, 1978).
[30] B.A. Aminov, A.A. Golubov, and M.Yu. Kupriyanov, Phys. Rev. B **53**, 365 (1996).
[31] A.V. Zaitsev and D.V. Auerin, Phys. Rev. Lett. **80**, 3602 (1998).
[32] J.R. Kirtley, Int. J. Mod. Phys. B **4**, 201 (1990).
[33] B.A. Aminov, M.A. Hein, G. Müller, H. Piel, D. Wehler, Y.G. Ponomarev, K. Rosner, and K. Winzer, J. Supercond. **7**, 361 (1994).
[34] N. Hass, D. Ilzycer, G. Deutscher, G. Desgardin, I. Monot, and M. Weger, J. Supercond. **5**, 191 (1992).
[35] K. Flensberg, J. B. Hansen, and M. Octavio, Phys. Rev. B **38**, 8707 (1988).
[36] A.A. Abrikosov, Physica C **182**, 191 (1991).
[37] W.A. Atkinson and J.P. Carbotte, Phys. Rev. B **52**, 10 601 (1995).
[38] V.Z. Kresin and S.A. Wolf, Phys. Rev. B **46**, 6458 (1992).
[39] W. Atkinson, J.P. Carbotte, and C. Donovan, Turk. J. Phys. **20**, 670 (1996).
[40] L. Alff, A. Beck, R. Gross, A. Marx, S. Kleefisch, Th. Bauch, H. Sato, M. Naito, and G. Koren, Phys. Rev. B **58**, 11 197 (1998).
[41] J.W. Ekin, Y. Xu, S. Mao, T. Venkatesan, D.W. Face, M. Eddy, and S.A. Wolf, Phys. Rev. B **56**, 13 746 (1997).
[42] A. Andreone, A. Cassinese, A. Di Chiara, R. Vaglio, A. Gupta, and E. Sarnelli, Phys. Rev. B **49**, 6392 (1994).
[43] L. Antognazza, K. Char, and T.H. Geballe, Appl. Phys. Lett. **68**, 1009 (1995).
[44] J. Appelbaum, Phys. Rev. Lett. **17**, 91 (1966); Phys. Rev. **154**, 633 (1967); P.W. Anderson, Phys. Rev. Lett. **17**, 95 (1966).
[45] M. Covington, M. Aprili, E. Paraoanu, L.H. Greene, F. Xu, J. Zhu, and C.A. Mirkin, Phys. Rev. Lett. **79**, 277 (1997).
[46] C.R. Hu, Phys. Rev. Lett. **72**, 1526 (1994).
[47] M. Fogelström, D. Rainer, and J.A. Sauls, Phys. Rev. Lett. **79**, 281 (1997).